LAB1 Report

Pin-Jing, Li (111511015 *ouo.ee11@nycu.edu.tw)*
Jing-Kai, Huang
Duan-Kai, Wu

September 17, 2025

In lab 1 We explored the basic configuration of e^2 studio, ultrasound module and the basic signal processing flow of the wireless transmitted signal.

1 Hardware configuration

2 Error Source Analysis

We inspect the relative distance and try to determine the model of the error.

Pair (cm)	n^*_{theory}	n_{meas}	$\Delta n^*_{\text{theory}}$	Δn_{meas}	$\frac{\Delta n_{\text{meas}}}{\Delta n^*_{\text{theory}}}$	Relative Error (%)
20→40	184.97→369.94	231→412	184.97	181	0.979	-2.1
40→60	369.94→554.91	412→598	184.97	186	1.006	+0.6
60→80	554.91→739.88	598→773	184.97	175	0.946	-5.4
80→100	739.88→924.86	773→953	184.97	180	0.973	-2.7

Table 1: Relative Distance Comparison (Measured vs. Theoretical)

We retrieve back n_{meas} by aligning the starting sample by the maximum Tx data
We plot out the

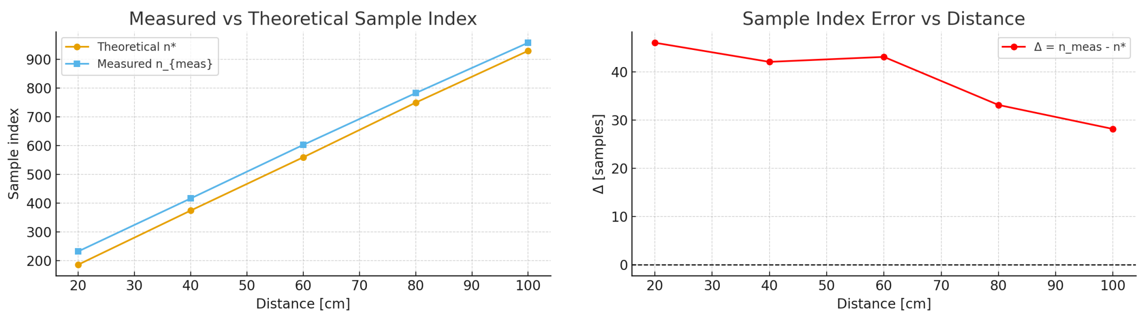

(a) Measured Peak and the theoretical sample (T=25)

(b) Error vs. distance

Figure 1: Comparing robust and non-robust design for linear precoder

$$\Delta = a + bn_{\text{meas}}$$

With linear regression we found $a \simeq 53.14, b \simeq -0.02469$, and we therefore perform the correction on the measurements

3 Signal Processing

some discussion below:

True Distance (cm)	n_{meas}	$\hat{n}$ (Corrected)	n^* (Theory)	Error After Correction (cm)
20	231	183.56	184.97	-0.15
40	412	369.04	369.94	-0.10
60	598	559.39	554.91	$+0.48$
80	773	738.65	739.88	-0.13
100	953	922.23	924.86	-0.28

Table 2: Corrected Sample Index and Residual Distance Error (Linear Model)

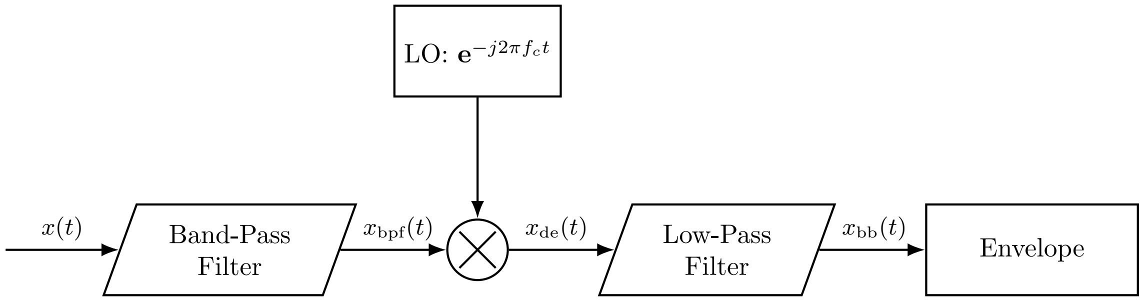

Figure 2: block diagram: signal → BPF → demod (mixer) → LPF → envelope.

- **Correct "Detection" threshold.** The physically correct measure of the time of flight (TOF) would be the *wavefront* of the received signal.

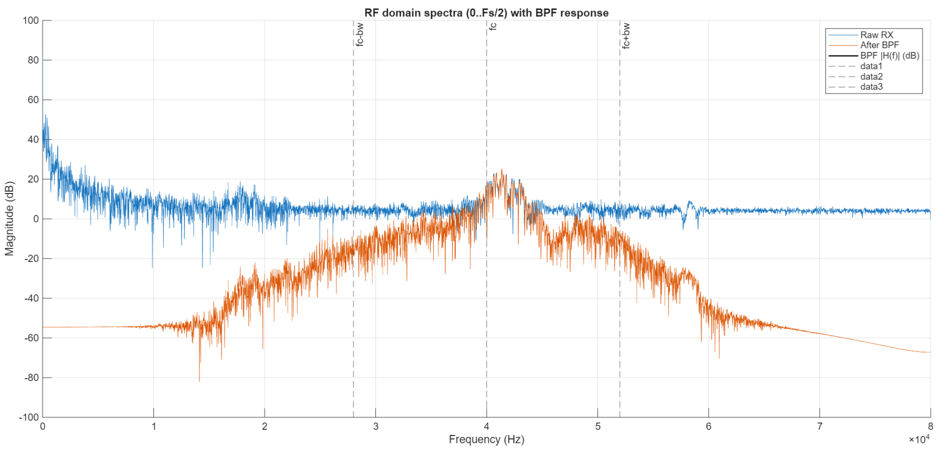

Figure 3: bpf

Bandpass Filtering

Given the sampled received signal $x(t)$, we first apply a bandpass filter to isolate the signal components near the carrier frequency. The bandpass-filtered signal is

$$x_{\text{bpf}}(t) = x(t) * h_{\text{bpf}}(t) \tag{1}$$

where $*$ denotes convolution and $h_{\text{bpf}}(t)$ is the impulse response of the bandpass filter.

Filter Design. We choose a 6^{th}-order IIR Butterworth bandpass filter with half-power frequencies

$$f_{\text{bp},1} = f_c - 2f_w, \qquad f_{\text{bp},2} = f_c + 2f_w,$$

where the carrier frequency $f_c = 40$ kHz and the signal bandwidth is

$$f_w = \frac{1}{T_{\text{burst}}} \approx 5 \text{ kHz}.$$

To ensure the filter design remains within valid frequency bounds, we compute:

$$\texttt{bp\_bw} = \max\left(2f_w,\ 12\ \text{kHz}\right),$$
$$\texttt{bp\_f1} = \max\left(10,\ f_c - \texttt{bp\_bw}\right),$$
$$\texttt{bp\_f2} = \min\left(\tfrac{F_s}{2} - 10,\ f_c + \texttt{bp\_bw}\right),$$

where F_s is the sampling frequency.

MATLAB Implementation. The filter is implemented and applied using MATLAB as follows:

```
bp_bw = max(2*fw, 12e3); % Bandwidth selection
bp_f1 = max(10, fc - bp_bw); % Lower cutoff frequency
bp_f2 = min(Fs/2-10, fc + bp_bw); % Upper cutoff frequency

dbp = designfilt('bandpassiir','FilterOrder',6, ...
    'HalfPowerFrequency1', bp_f1, ...
    'HalfPowerFrequency2', bp_f2, ...
    'SampleRate', Fs);

rx_bp = filtfilt(dbp, rx_dc); % Zero-phase filtering
```

This produces the zero-phase bandpass-filtered signal $x_{\text{bpf}}(t)$.

Demodulation

After bandpass filtering, we demodulate the signal by multiplying it with a complex exponential at the carrier frequency f_c:

$$x_{\text{de}}(t) = x_{\text{bpf}}(t) \cdot e^{-j2\pi f_c t} \tag{2}$$

In the frequency domain, this shifts the bandpass signal to baseband, centering its spectrum around 0 Hz.

```
w0 = 2*pi*fc/Fs; % Normalized carrier frequency (rad/sample)
lo = exp(-1j*w0*n); % Complex exponential for downconversion
bb = rx_bp .* lo; % Complex baseband signal
```

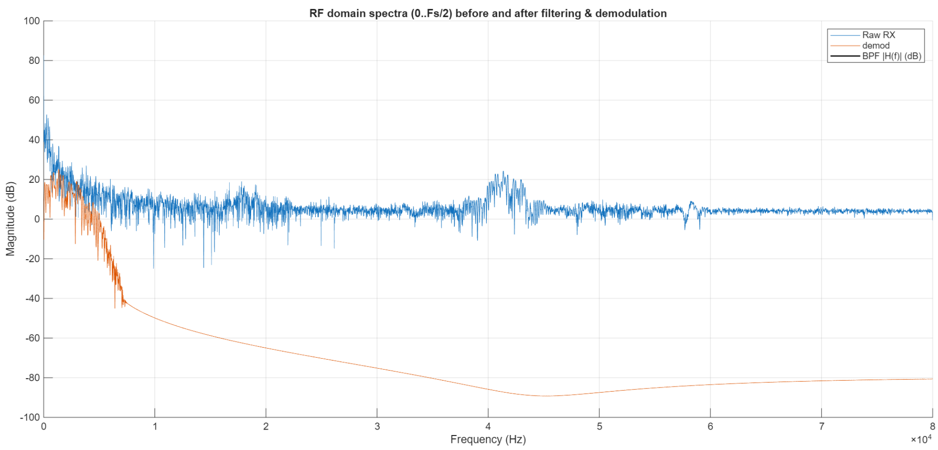

Figure 4: demod

—

Low-Pass Filtering

The downconverted signal still contains high-frequency components due to the product term. We pass $x_{\text{de}}(t)$ through a low-pass filter to retain only the baseband component.

Filter Design. We use a FIR low-pass filter with passband edge at $f_{\mathrm{LP}} = f_c$ and stopband starting at $1.6 f_{\mathrm{LP}}$:

```
% FIR: passband up to lp_fc, stopband starts at 1.6*lp_fc
dlp = designfilt('lowpassfir', ...
    'PassbandFrequency', lp_fc, ...
    'StopbandFrequency', 1.6*lp_fc, ...
    'PassbandRipple', 0.1, ...
    'StopbandAttenuation', 70, ...
    'SampleRate', Fs);

bb_f = filtfilt(dlp, real(bb)) + 1j*filtfilt(dlp, imag(bb));
```

This yields the complex baseband signal $x_{\mathrm{bb}}(t)$ with high-frequency components removed.
—

Envelope Detection

Since the original signal is carried by f_c, it can be expressed as

$$x(t) = A\cos(2\pi f_c t + \phi).$$

After demodulation, we have

$$\mathrm{Re}\{x_{\mathrm{de}}(t)\} = x(t)\cos(2\pi f_c t) = \frac{A}{2}\big[\cos(\phi) + \cos(4\pi f_c t + \phi)\big].$$

Thus, the envelope amplitude is halved. We compensate for this loss by multiplying by 2 when extracting the magnitude of the analytic signal:

```
env = 2 * abs(bb_f);
```

This produces the envelope of the baseband signal, scaled back to its original amplitude.

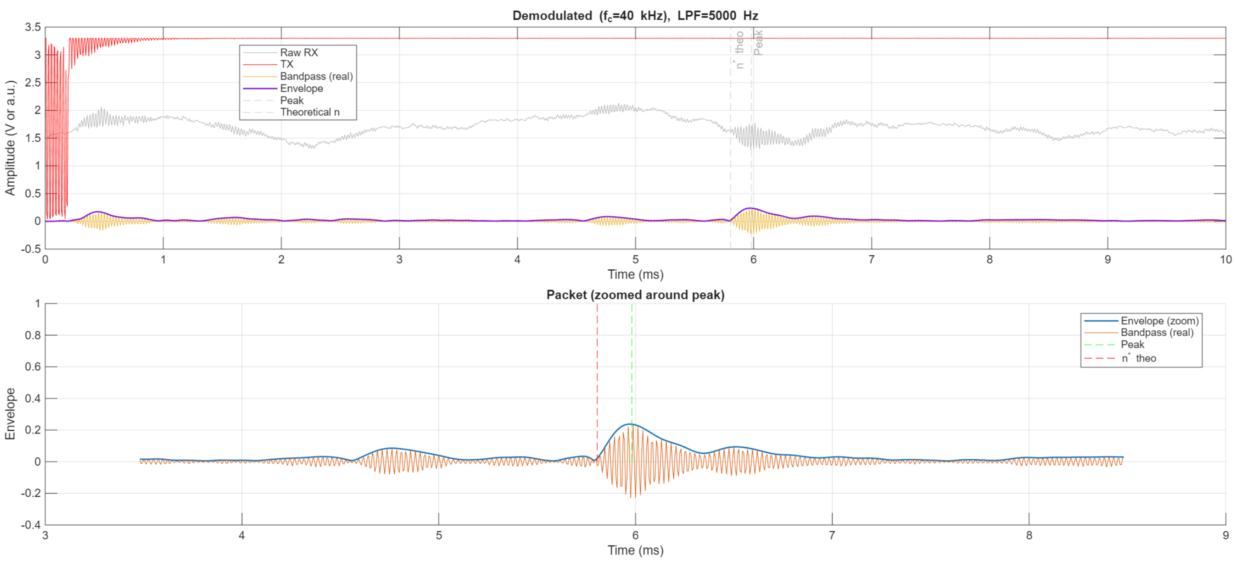

Figure 5: Time domain signal before and after filtering & demodulation

References

[1] C.-Y. Chang and C.C. Fung, "Sparsity enhanced mismatch model for robust spatial intercell interference cancelation in heterogeneous networks," *IEEE Trans. on Communications*, vol. 63(1), pp. 125-139, Jan. 2015.

[2] I. P. Roberts, Y. Zhang, T. Osman, and A. Alkhateeb, "Real-world evaluation of full-duplex millimeter wave communication systems," *IEEE Trans. Wireless Commun.*, early access, Mar. 2024.

[3] K. Shen and W. Yu, "Fractional Programming for Communication Systems—Part I: Power Control and Beamforming," *IEEE Transactions on Signal Processing*, vol. 66, no. 10, pp. 2616-2630, May 15, 2018, doi: 10.1109/TSP.2018.2812733.

[4] J. Ho, A. Jain, and P. Abbeel, "Denoising diffusion probabilistic models," *Advances in Neural Information Processing Systems*, vol. 33, pp. 6840–6851, 2020.

[5] T. O'Shea and J. Hoydis, "An introduction to deep learning for the physical layer," *IEEE Transactions on Cognitive Communications and Networking*, vol. 3, no. 4, pp. 563–575, 2017.

[6] M. Servetnyk and C. C. Fung, "Distributed fronthaul-constrained joint transmission design and selection using augmented consensus-based dual decomposition," *Journal of Communications and Networks*, vol. 24, no. 4, pp. 419–437, Aug. 2022, doi: 10.23919/JCN.2022.000030.